Proceedings of the
47th IEEE Conference on Decision and Control
Cancun, Mexico, Dec. 9-11, 2008

Consensus Filter Based Target-enclosing Strategies for Multiple Nonholonomic Vehicles

Hiroki Kawakami and Toru Namerikawa

***Abstract*— This paper deals with cooperative target-enclosing problems using consensus filter for multiple vehicle systems. Proposed strategies are based on consensus seeking algorithms and at least one vehicle only has to acquire the states of target-object. In addition, the measurement signals are made to be agreed using the consensus filters when each vehicle acquires the noisy signal of the states of the target-object. To analyze the enclosing problem, algebraic graph theory and matrix theory are utilized. Numerical simulations and experiments are carried out to demonstrate the effectiveness of proposed methods.**

I. INTRODUCTION

In recent years, there have been increasing research interests in the distributed cooperative control of multi-vehicle systems [1]-[3]. Several research groups developed the coordination control strategies that achieve a capturing formation around a target-object (specific area) by multiple mobile vehicles using local information [4]-[10]. Owing to the broad range of applications ($e.g.$ investigations in hazardous environments, mobile sensor networks and security systems), the task of capturing target-object is investigated in the distributed cooperative control of multi-vehicle systems.

The capturing the target-object is divided into two problems, grasping behavior and enclosing behavior. The grasping behavior is the object-closure condition in decentralized form in [4]. On the other hand, the enclosing behavior is that multiple vehicles are controlled in a distributed manner to converge to an assigned formation while tracking the target-object. Kobayashi *et al.* [6] proposed the decentralized grasping control law using the concept of force-closure and enclosing control law based on a gradient decent method for multiple vehicles with local information in a plane. In their method, each vehicle requires local information of target-object and two neighbor vehicles. Marshall *et al.* [11] proposed a cyclic pursuit based formation control strategies for multiple mobile vehicles moving in a plane. They showed that the multiple vehicles finally can assemble in a circular formation that is similar to that of [6]. In [5], Kim *et al.* proposed a distributed cooperative control method based on a cyclic pursuit strategy in a target-enclosing task in $3\mathcal{D}$ space by multi-vehicle systems. In the above method, each vehicle's behavior is decided using the information of target-object and one neighbor vehicle. In [5][6], however, enclosing strategies for multiple vehicles with nonholonomic constraints ($e.g.$ two-wheeled vehicles and AUVs) have not been considered and in their method, all vehicles require the information of the target-object. In addition, the information exchange topologies among the vehicles are limited to the cycle graphs. $i.e.$ enclosing the target-object cannot be achieved with the information exchange topologies except cycle graphs. Consensus algorithm based formation control strategies for multi-vehicle systems are proposed in [12]-[15]. Ren [13] proposed the formation control strategies for multi-vehicle systems where the information states of each vehicle approach a common time-varying reference state. Similarly, Namerikawa *et al.* [14][15] proposed a formation control strategies based on consensus algorithm for multi-vehicle systems.

H. Kawakami and T. Namerikawa are with Division of Electrical Engineering and Computer Science, Graduate School of Natural Science and Technology, Kanazawa University, Kakuma-machi, Kanazawa 920-1192 JAPAN. hiroki@scl.ec.t.kanazawa-u.ac.jp and toru@t.kanazawa-u.ac.jp

Most consensus algorithm results related to cooperative control are obtained for linear vehicles. However, most practical cooperative control applications involve systems that are nonlinear and nonholonomic. Therefore, it is necessary to discuss cooperative control of nonholonomic vehicles. There have been some previous research works [9], [14], [15], [16] which treated cooperative control of multiple nonholonomic vehicles.

In many networked vehicle applications, it is important for vehicles to have a global aggregate of the network's vehicle measurement. Consensus filtering [17]-[19] provides one way of computing such aggregates in a distributed manner. The role of the consensus filter is to perform distributed fusion of sensor measurements. Generally, if the density of the network and filter gain are large, this filter decreases the influence of the noise.

In this paper, we propose target-enclosing strategies using consensus filter for multiple nonholonomic vehicles which are controlled to converge to the formation while they are tracking the target-object moving in a plane. We first define a virtual vehicle in each vehicle to apply the consensus seeking algorithm to nonholonomic vehicle, and linearize each vehicle. We propose the enclosing control law based on the consensus seeking algorithm to each virtual vehicle. Then, the target-object is enclosed using the states of the consensus filter for the control law. Finally, the effectiveness of the proposal method is verified by the numerical simulations and experiments.

This paper is organized as follows. Section II introduces preliminaries (algebraic graph theory). Section III introduces the virtual structures corresponding to real vehicles and real target-object respectively and control objectives of the enclosing behavior. Section IV describes the proposed enclosing strategies for multiple nonholonomic vehicles. Section V describes the proposed enclosing strategies using

978-1-4244-3124-3/08/$25.00 ©2008 IEEE

consensus filters for multiple nonholonomic vehicles. In Section VI, we validate our results by numerical simulations and experiments. Finally, we summarize the obtained results in Section VII.

II. Preliminaries

Information exchange between vehicles or between the vehicle and the target-object can be represented as a graph. We give here some basic some terminology and definitions from graph theory. Let $\mathscr{G} = (\mathscr{V}, \mathscr{E})$ denoted a graph with the set of vertices $\mathscr{V} = \{1, 2, \cdots, n\}$ and the set of edges $\mathscr{E} \subseteq \mathscr{V} \times \mathscr{V}$. The graph is divided into undirected graphs and directed graphs (digraphs). The set of neighbors of vertex i is denoted by

$$\mathcal{N}_i = \{j \in \mathscr{V} : (j, i) \in \mathscr{E}\}. \tag{1}$$

An undirected graph is called connected if there is an edge between any distinct pair of vertices. A directed graph is called strongly connected if there is a directed path from every vertex to every other vertex. A directed tree is a directed graph, where every vertex has exactly one parent except for one vertex, called root, which has no parent, and the root has a directed path to every other vertex [13]. Note that in a directed tree, each edge has a natural orientation away from the root, and no cycle exists. In the case of undirected graphs, a tree is a graph in which every pair of vertices is connected by exactly one path. A directed spanning tree of a directed tree formed by graph edges that connect all of the vertices of the graph. Note that the condition that a digraph has a directed spanning tree is equivalent to the case that there exists as least a vertex having a directed path to all of the other vertices. In the case of undirected graphs, having an undirected spanning tree is equivalent to being connected. A graph in which every vertex has equal valency k is called k-regular.

The adjacency matrix $\mathcal{A}_n(\mathscr{G}) = [a_{ij}] \in \mathbb{R}^{n \times n}$ is defined as $a_{ii} = 0$ and $a_{ij} = 1$ if $(j, i) \in \mathscr{E}$ where $i \neq j$. The adjacency matrix of a undirected graph is defined accordingly except that $a_{ij} = a_{ji}, {}^\forall i \neq j$, since $(j, i) \in \mathscr{E}$ implies $(i, j) \in \mathscr{E}$. The degree of vertex i is the number of its neighbors $|\mathcal{N}_i|$ and is denoted by deg(i). The degree matrix of graph $\mathscr{G}$ is diagonal matrix defined as $\mathcal{D}_n(\mathscr{G}) = [d_{ij}] \in \mathbb{R}^{n \times n}$ where

$$d_{ij} = \begin{cases} \deg(i) & , i = j \\ 0 & , i \neq j \end{cases} \tag{2}$$

Laplacian matrix of the graph $\mathscr{G}$ is defined by

$$\mathcal{L}_n(\mathscr{G}) = \mathcal{D}_n(\mathscr{G}) - \mathcal{A}_n(\mathscr{G}) = [l_{ij}] \in \mathbb{R}^{n \times n} \tag{3}$$

For an undirected graph, the Laplacian matrix $\mathcal{L}_n$ is symmetric positive semi-definite. This property does not hold for a digraph Laplacian matrix. An important feature of $\mathcal{L}_n$ is that all the row sums of $\mathcal{L}_n$ are zero and thus $\mathbf{1} = \begin{bmatrix} 1 & 1 & \cdots & 1 \end{bmatrix}^T \in \mathbb{R}^n$ is eigenvector of $\mathcal{L}_n$ associated with the eigenvalue $\lambda(\mathcal{L}_n) = 0$.

III. Problem Formulation

A. Nonholonomic Vehicles and Target-object

In this subsection, we consider N nonholonomic mobile vehicles (see the lower left at Figure 1(a)). i^{th} nonholonomic mobile vehicle is modeled by the following nonlinear ordinary differential equations

$$\begin{bmatrix} \dot{x}_i \\ \dot{y}_i \\ \dot{\theta}_i \end{bmatrix} = \begin{bmatrix} \cos\theta_i & 0 \\ \sin\theta_i & 0 \\ 0 & 1 \end{bmatrix} \begin{bmatrix} v_i \\ \omega_i \end{bmatrix} \tag{4}$$

where $r_i = [x_i \ y_i]^T \in \mathbb{R}^2$ is the position of i^{th} vehicle, $\theta_i \in [0, 2\pi)$ is the orientation, $v_i \in \mathbb{R}$ is the linear velocity and $\omega_i \in \mathbb{R}$ is the angular velocity. The vehicles have the following nonholonomic constraint of pure rolling and non-slipping.

$$\dot{x}_i \sin\theta_i - \dot{y}_i \cos\theta_i = 0 \tag{5}$$

We define the *virtual vehicle* (see the upper right at Figure 1(a)) corresponding to the real vehicle (4). Then, the relation between i^{th} real vehicle and i^{th} virtual vehicle is given by

$$\begin{bmatrix} x_{vvi} \\ y_{vvi} \\ \theta_{vvi} \end{bmatrix} = \begin{bmatrix} x_i + \alpha\cos\theta_i - \beta\sin\theta_i \\ y_i + \alpha\sin\theta_i + \beta\cos\theta_i \\ \theta_i \end{bmatrix}, \tag{6}$$

where $r_d = [\alpha \ \beta]^T \in \mathbb{R}^2$ is relative distance between real vehicle and virtual vehicle, $r_{vvi} = [x_{vvi} \ y_{vvi}]^T \in \mathbb{R}^2$ and $\theta_{vvi} \in [0, 2\pi)$ are, respectively, the position, the orientation of i^{th} virtual vehicle. Then, the derivative of eq. (6) is given as

$$\left[\begin{array}{c} \dot{x}_{vvi} \\ \dot{y}_{vvi} \\ \hline \dot{\theta}_{vvi} \end{array}\right] = \left[\begin{array}{c} B_i \\ \hline B_\theta \end{array}\right] \begin{bmatrix} v_i \\ \omega_i \end{bmatrix} \tag{7}$$

where $[v_i \ \omega_i]^T \in \mathbb{R}^2$ is the control input to i^{th} vehicle and

$$B_i = \begin{bmatrix} \cos\theta_i & -\alpha\sin\theta_i - \beta\cos\theta_i \\ \sin\theta_i & \alpha\cos\theta_i - \beta\sin\theta_i \end{bmatrix}, \tag{8}$$

$$B_\theta = \begin{bmatrix} 0 & 1 \end{bmatrix}. \tag{9}$$

Here, we construct the following control input $\begin{bmatrix} v_i & \omega_i \end{bmatrix}^T$.

$$\begin{bmatrix} v_i \\ \omega_i \end{bmatrix} = B_i^{-1} u_i \tag{10}$$

If we assume $\alpha \neq 0$, B_i is a non-singular matrix.

Now, we consider the following target-object.

$$\dot{r}_{obj} = f(t, r_{obj}) \tag{11}$$

where $r_{obj} = [x_{obj} \ y_{obj}]^T \in \mathbb{R}^2$ is the position of target-object. The target-object satisfies the following assumtion.

Assumption 1 *$\dot{r}_{obj}$ is piecewisely continuous in t and locally Lipschitz in r_{obj}.*

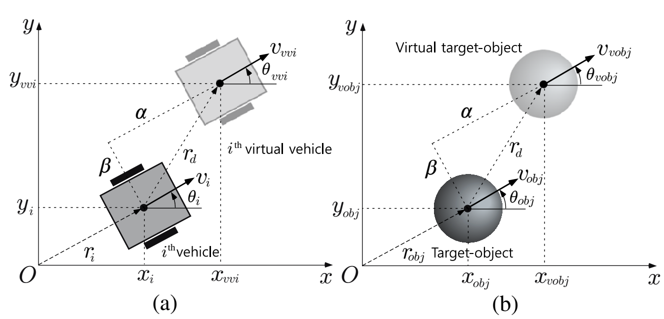

Fig. 1. (a) Real vehicle and virtual vehicle, (b) Real target-object and virtual target-object.

Similarly, we consider the virtual target-object corresponding to real target-object (see Figure 1(b)). Then, the states of virtual target-object are given as well as the case of virtual vehicles as follows

$$\begin{bmatrix} x_{vobj} \\ y_{vobj} \\ \theta_{vobj} \end{bmatrix} = \begin{bmatrix} x_{obj} + \alpha\cos\theta_{obj} - \beta\sin\theta_{obj} \\ y_{obj} + \alpha\sin\theta_{obj} + \beta\cos\theta_{obj} \\ \theta_{obj} \end{bmatrix}, \quad (12)$$

where $r_{vobj} = [x_{vobj}\ y_{vobj}]^T \in \mathbb{R}^2$ is the position of virtual target-object, $\theta_{obj} \in [0, 2\pi)$ is the moving orientation of real target-object and $\theta_{vobj} \in [0, 2\pi)$ is the moving orientation of virtual target-object.

B. Control Objectives

We first define the position in which i^{th} vehicle encloses the target-object as *enclosing position* $R_i \in \mathbb{R}^2$. Note that for the sake of clarity and page limitation, this paper only considers the equal convergence positions for all vehicles; *i.e.*,

$$\|R_1\| = \|R_2\| = \cdots = \|R_n\| = \xi \quad (13)$$

where $\xi \in \mathbb{R}$ is the *enclosing radius* and $\|\cdot\|$ is the Euclidean norm. Let $\phi_{vvi} \in \mathbb{R}$ denotes the counterclockwise angle of i^{th} virtual vehicle and the center is the virtual target-object. We also define the following target-enclosing behavior.

Definition 1 *(target-enclosing behavior)*
The $N \geq 2$ vehicles are spaced out around the target-object at intervals of the assigned angles and maintain these angles and each vehicle approaches to the target-object and finally keeps the distance ξ.

In other words, control objectives for virtual structure based target-enclosing behavior can be formulated as follows (see Figure 2) ;

C1) $\lim_{t\to\infty} \|r_{vvi}(t) - r_{vobj}(t)\| = \xi$ [m],
C2) $\lim_{t\to\infty} \|\phi_{vv(i+1)}(t) - \phi_{vvi}(t)\| = \frac{2\pi}{N}$ [rad],
C3) $\lim_{t\to\infty} \|\theta_{vvi}(t) - \theta_{vobj}(t)\| = 0$ [rad],

$$i, j = 1, 2, \cdots, N \ (i \neq j).$$

If $i = N$, then $N + 1 = 1$.

In the next section, the target-enclosing strategy which achieves the objectives C1)-C3) is developed.

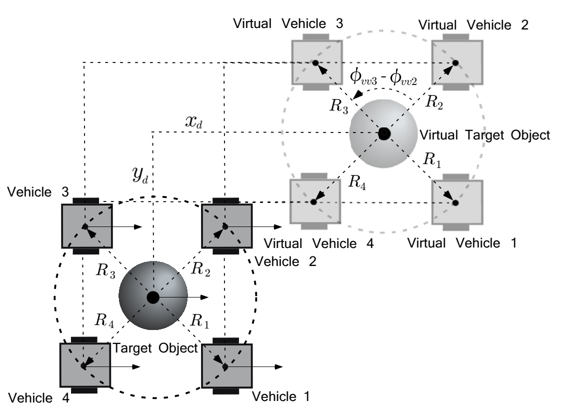

Fig. 2. An example of target-enclosing behavior by $N = 4$ virtual vehicles

IV. Virtual Structure Based Target Enclosing Strategies

In this subsection, we discuss the case that a portion of vehicles have access to the target-object (*i.e.* the leader-follower systems). It is assumed that it is generally difficult to get the information of the target-object in actual environment. Here, we make the following *Assumptions 1-2*.

Assumption 2 *: Target-object are included in the network topology which has a spanning tree.*

Assumption 3 *: The target-object moves at the linear velocity $v_{obj} = \|\dot{r}_{obj}\| \neq 0, {}^\forall t \geq 0$, the leaders can acquire the position r_{obj} of target object and its derivative $\dot{r}_{obj}$. i^{th} follower can acquire the position r_{vvj} of the neighbor j^{th} follower and its derivative $\dot{r}_{vvj}$.*

We propose the target-enclosing control laws based on [13][15]. Here, we call that leader-vehicles with direct access to the target-object. Conversely, we call that follower-vehicles without direct access to the target-object.

The proposed control laws for the leader-vehicles and follower-vehicles are described as

- Control input for the leader-vehicles

$$u_i = \frac{1}{1+\sum_{j=1}^N a_{ij}} \Big[-k_i\left(\hat{r}_{vvi} - r_{vobj}\right) + \dot{r}_{vobj} + \dot{R}_i + \sum_{j=1}^N a_{ij} \left\{ -k_i\left(\hat{r}_{vvi} - \hat{r}_{vvj}\right) + \dot{r}_{vvj} + \dot{R}_{ij} \right\} \Big] \quad (14)$$

- Control input for the follower-vehicles

$$u_i = \frac{1}{\sum_{j=1}^N a_{ij}} \left[\sum_{j=1}^N a_{ij} \left\{ -k_i\left(\hat{r}_{vvi} - \hat{r}_{vvj}\right) + \dot{r}_{vvj} + \dot{R}_{ij} \right\} \right] \quad (15)$$

where $k_i \in \mathbb{R}$ is controller gain, $R_{ij} = R_i - R_j$ and $\hat{r}_{vvi} = r_{vvi} - R_i$. Now, we design enclosing position R_i as follows

$$R_i = \xi \begin{bmatrix} \cos\frac{2\pi(i-1)}{N} & \sin\frac{2\pi(i-1)}{N} \end{bmatrix}^T. \quad (16)$$

Here, we have the following *Theorem 1*.

Theorem 1 *: Consider the system of N virtual vehicles (7) and the virtual target-object (12). We apply the enclosing control law (14)(15)(16) to the system. If the system satisfies $k_i > 0$ and Assumption 1-3, then the system asymptotically achieves the control objectives C1)-C2).*

Proof: For (14)(15), let $r_{obj} \doteq \hat{r}_{N+1}$, $r_{vobj} \doteq \hat{r}_{vv(N+1)}$. We rewrite Eq. (14)(15) as

$$\sum_{j=1}^{N+1} a_{ij} \left(\dot{\hat{r}}_{vvi} - \dot{\hat{r}}_{vvj} \right) = -k_i \sum_{j=1}^{N+1} a_{ij} \left(\hat{r}_{vvi} - \hat{r}_{vvj} \right). \quad (17)$$

Eq. (17) can be written in matrix form as $\left(\mathcal{L}_{N+1} \otimes I_2\right)\dot{\hat{r}}_{vv} = -k_i\left(\mathcal{L}_{N+1} \otimes I_2\right)\hat{r}_{vv}$, which implies that $\hat{r}_{vvi} \to \hat{r}_{vvj}$, $\hat{r}_{vvi} \to r_{vobj}$ *as* $t \to \infty, {}^\forall i$, since $\hat{r}_{vv(N+1)} \doteq r_{vobj}$, $\otimes$ is kronecker products and $\hat{r}_{vv} = [\ \hat{r}_{vv1}^T \ \ \hat{r}_{v21}^T \ \cdots \ \hat{r}_{vv(N+1)}^T\ ]^T$. Therefore,

$$r_{vvi} - r_{vvj} \ \to\ R_{ij} \quad as \quad t \to \infty, \quad (18)$$

$$r_{vvi} - r_{vobj} \ \to\ R_i \quad as \quad t \to \infty. \quad (19)$$

From Eq. (16), we represent $R_i = \xi e^{j\frac{2\pi}{N}(i-1)} \in \mathbb{R}^2 \approx \mathbb{C}$, $\|R_i\| = \xi$ and

$$R_{i+1} = e^{j\frac{2\pi}{N}} R_i \tag{20}$$

Consequently, we obtain

$$\|r_{vvi} - r_{vobj}\| \to \xi \ [\mathrm{m}] \quad as \ t \to \infty \tag{21}$$

and

$$\|\phi_{vv(i+1)} - \phi_{vvi}\| \to \frac{2\pi}{N} \ [\mathrm{rad}] \ as \ t \to \infty. \tag{22}$$

Therefore, if we design the enclosing position R_i(16), then the system achieves the control objectives C1)-C2). ■

Proposition 1 *: The steady orientation of virtual target-object is assumed as $\dot{\theta}_{obj} = \dot{\theta}_{vobj} = 0$. Then, the orientations of all virtual vehicles achieve the orientation of virtual target-object. i.e. $\theta_{vvi} \to \theta_{vobj}$ as $t \to \infty, {}^\forall i \in \mathscr{V}$.*

Proof: From Eq. (7), the orientation of i^{th} virtual vehicle is given by

$$\dot{\theta}_{vvi} = B_\theta B_i^{-1} u_i. \tag{23}$$

From Eq. (14) and Eq. (15), the derivative of the orientation of i^{th} virtual vehicle is given by

$$\dot{\theta}_{vvi} = -\frac{1}{\sum_{j=1}^{N+1} a_{ij} x_d} \left\{ \sum_{j=1}^{N+1} a_{ij} \|\dot{r}_j\| \sin(\theta_{vvi} - \theta_{vvj}) \right\}, \tag{24}$$

which implies that $\theta_{vvi} \to \theta_{vvj}$, $\theta_{vvi} \to \theta_{vobj}$ as $t \to \infty$. ■

From *Theorem 1* and *Proposition 1*, the control objectives C1)-C3) are achieved. Next, we consider the enclosing position is changed according to the speed of the target-object. It is the same as the Eq. (16) when the speed of the target-object is very slow. The vehicle concentrates on the moving direction when the speed of the target-object is fast. If the speed of target-object is fast, then $\|\phi_{vv(i+1)} - \phi_{vvi}\| \neq \frac{2\pi}{N}$.

Proposition 2 *: Consider the system of N virtual vehicles (7) and the virtual target-object (12). We apply the target-enclosing control law (14)(15) and the following enclosing position*

$$R_i \triangleq \chi \begin{bmatrix} \cos\left\{ \dfrac{2\pi(i-1)}{N} e^{-k_r \sum\limits_{j=1}^{N+1} a_{ij} \|\dot{r}_{vvj}(t)\|} \right\} \\ \sin\left\{ \dfrac{2\pi(i-1)}{N} e^{-k_r \sum\limits_{j=1}^{N+1} a_{ij} \|\dot{r}_{vvj}(t)\|} \right\} \end{bmatrix}^T, \tag{25}$$

$$\chi \triangleq \xi \begin{bmatrix} \cos\sum_{j=1}^{N+1} a_{ij}\theta_{vvj} & -\sin\sum_{j=1}^{N+1} a_{ij}\theta_{vvj} \\ \sin\sum_{j=1}^{N+1} a_{ij}\theta_{vvj} & \cos\sum_{j=1}^{N+1} a_{ij}\theta_{vvj} \end{bmatrix}, \tag{26}$$

where $k_r > 0 \in \mathbb{R}$ is constant gain. If the system satisfies $k_i > 0$ and Assumption 1-2, then the system asymptotically achieves the control objective C1).

Proof: For Eq. (14)(15), let $r_{vobj} \doteq \hat{r}_{vv(N+1)}$. Eq. (17) can be written in matrix form as $(\mathcal{L}_{N+1} \otimes I_2)\dot{\hat{r}}_{vv} = -k_i(\mathcal{L}_{N+1} \otimes I_2)\hat{r}_{vv}$, which implies that $\hat{r}_{vvi} \to \hat{r}_{vvj}$, $\hat{r}_{vvi} \to r_{vobj}$, ${}^\forall i$, since $\hat{r}_{vv(N+1)} \doteq r_{vobj}$. Therefore,

$$r_{vvi} - r_{vvj} \quad \to \quad R_{ij} \quad as \quad t \to \infty, \tag{27}$$
$$r_{vvi} - r_{vobj} \quad \to \quad R_i \quad as \quad t \to \infty. \tag{28}$$

From (25)(26), we represent $\|R_i\| = \xi$. Consequently, we obtain

$$\|r_{vvi} - r_{vobj}\| \to \xi \ [\mathrm{m}] \quad as \ t \to \infty \tag{29}$$

Therefore, if we design the control laws (14)(15) and the enclosing position R_i (25), then the system asymptotically achieves the control objective C1). ■

Remark 1 *Eq. (25)(26) can be expressed if the speed of target-object is very slow ($v_{vobj} \approx 0$) as the following enclosing position.*

$$R_i \approx \chi \begin{bmatrix} \cos\left(\frac{2\pi(i-1)}{N}\right) & \sin\left(\frac{2\pi(i-1)}{N}\right) \end{bmatrix}^T \tag{30}$$

In addition, Eq. (25)(26) can be expressed if the speed is fast of target-object ($v_{vvj} \gg 0$) as the following enclosing position.

$$R_i \approx \chi \begin{bmatrix} 1 & 0 \end{bmatrix}^T \tag{31}$$

V. Target-Enclosing Behavior with Consensus Filter

We assume each vehicle is measuring a signal that is corrupted by noise w_i that is a zero-mean white Gaussian noise. Hence, the measurement model is as follows.

$$\tilde{r}^i_{obj}(t) = r_{obj}(t) + w_i(t), \qquad i = 1, \cdots, m \tag{32}$$
$$\tilde{r}_{obj}(t) = \mathbf{1} \otimes r_{obj}(t) + w(t) \tag{33}$$

where $\tilde{r}^i_{obj} \in \mathbb{R}^2$ is the signal with noise, r_{obj} is real signal, $\mathbf{1} = \begin{bmatrix} 1 & 1 & \cdots & 1 \end{bmatrix}^T \in \mathbb{R}^m$, $w = \begin{bmatrix} w_1^T & w_2^T & \cdots & w_m^T \end{bmatrix}^T \in \mathbb{R}^{2m}$, $\tilde{r}_{obj} = \begin{bmatrix} \tilde{r}^{1T}_{obj} & \tilde{r}^{2T}_{obj} & \cdots & \tilde{r}^{mT}_{obj} \end{bmatrix}^T \in \mathbb{R}^{2m}$.

Next, we introduce the consensus filter based on [17]. The role of this consensus filter is to perform distributed fusion of vehicle's sensor measurements.

We introduce the following consensus filter.

$$\dot{x}^c_i = k_c \sum_{j \in \mathcal{N}_i} \left(x^c_j - x^c_i\right) + k_c \sum_{j \in \mathcal{J}_i} \left(\tilde{r}^j_{obj} - x^c_i\right) \tag{34}$$

where $x^c_i \in \mathbb{R}^2$ is the state of the filter in i^{th} vehicle, $k_c > 0 \in \mathbb{R}$ is the filter gain, $\mathcal{J}_i = \mathcal{N}_i \cup i$. Filter (34) can be expressed as

$$\dot{x}^c = -k_c(I_m + \mathcal{D}_m + \mathcal{L}_m) \otimes I_2 x^c + k_c(I_m + \mathcal{A}_m) \otimes I_2 \tilde{r}_{obj} \tag{35}$$

where $\mathcal{D}_m$ and $\mathcal{A}_m$ is degree matrix and adjacent matrix respectively. The transfer function of the consensus filter (35) is given by

$$\mathcal{H}(s) = k_c [sI_{2m} + k_c(I_m + \mathcal{D}_m + \mathcal{L}_m) \otimes I_2]^{-1} (I_m + \mathcal{A}_m) \otimes I_2 \tag{36}$$

From Gersgorin theorem, all poles of $\mathcal{H}(s)$ are strictly negative and fall within the interval

$$1 + d_{\min} \leq \lambda(I_m + \mathcal{D}_m + \mathcal{L}_m) \leq 1 + 3d_{\max} \tag{37}$$

with $d_{\min} \triangleq \min_i d_i$, $d_{\max} \triangleq \max_i d_i$ and λ is eigenvalue. Therefore consensus filter (35) is stable filter.

Lemma 1 *[17] : Let $r_{obj}(t)$ be a signal with a uniformly bounded rate $\|\dot{r}_{obj}(t)\| \leq \nu$. Then $\mathbf{1} \otimes r_{obj}$ is a globally asymptotically ϵ-stable equibrium of the dynamics of the consensus filter (35) and*

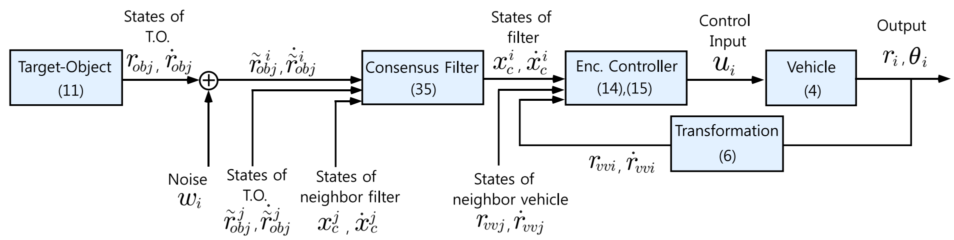

Fig. 3. Enclosing controller configuration using consensus filter

$$\epsilon = \frac{\nu\sqrt{m}}{k_c \lambda_{\min}(I_m + \mathcal{D}_m + \mathcal{L}_m)}. \tag{38}$$

If the density of the information exchange topology are large, the gain k_c are very large and the velocity of the target-object is very small ($\nu \approx 0$), then $\epsilon \approx 0$.

We consider the states x^c of the consensus filter (35) is replaced in the states r_{obj} of the target-object in Eq. (12). Therefore the control laws(14)(15) and control objectives C1)-C2) use the states x^c of the filter instead of the states of the target-object. Consensus filter is used only for leader agents. Moreover, the leader agents are connected with neighbor leaders.

Theorem 2 *: Consider the system of N virtual vehicles and the virtual target-object (12). We apply the enclosing control law (14)(15)(16) to the system. The states r_{obj} of the target-object are treated as states x_c of the consensus filter (35). If the system satisfies $k_i > 0, k_c > 0$ and Assumptions 1-3, then the system asymptotically achieves the control objectives C1)-C2).*

VI. Evaluation by Simulations and Control Experiments

In this section, we evaluate the performances of the target-enclosing strategies by the numerical simulations and experiments. Figure 4 shows the two kinds of the information exchange topologies.

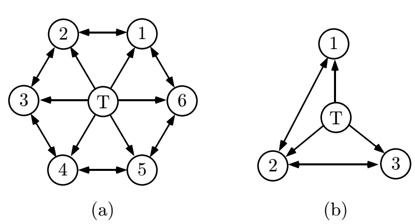

Fig. 4. Information exchange topologies

TABLE I

Control Parameters for Simulations

k_i	1.5
k_c	5
k_r	10
r_d [m]	[0.2, 0]
R_i [m]	$2\left[\cos\frac{\pi}{3}(i-1), \sin\frac{\pi}{3}(i-1)\right]$
Case 1 : v_{vobj} [m/s]	0.06
Case 2 : v_{vobj} [m/s]	0 → 0.06

A. Simulation Results

In this subsection, the performances of the target-enclosing strategies are evaluated by numerical simulations. To illustrate the enclosing performances of the proposed method, the simulations are carried out in which $N = 6$ vehicles described by Eq. (4) and a target-object with information exchange topology in Figure 4(a). The control parameters of the simulations are given as shown in Table I. And, we set the covariance of w_i ($W = 0.01 I_2$) for all i.

The simulation results are shown in Figures 6-7. Figure 6 illustrates the trajectories of six vehicles and the target-object using enclosing position (16). In figure 6, '$\times$' is the initial position of each virtual vehicle, '$\bullet$' is the final position of each virtual vehicle. Figure 7 illustrates trajectories of the six vehicles and the target-object using enclosing position (25). The speed of target-object is set as follow : $v_{obj} = 0.0012 * t, \ t \in [0, 50]$. These results show that all vehicles converge to a circular formation around the target-object. From the simulation results, the control objectives C1)-C3) are achieved.

B. Control Experimental Results

In experiments (see Figure 5, the four two-wheeled vehicles (nonholonomic vehicles) for vehicles and the same one vehicle for the target-object are used. The vehicles used in the experiments are controlled by a digital signal processor (DSP) from dSPACE Inc., which utilizes a PowerPC running at 3.2 [GHz]. Control programs are written in MATLAB/Simulink, and implemented on the DSP using the Real-Time Workshop and dSPACE software which includes ControlDesk, Real-Time Interface. A CCD camera is mounted above the vehicles. The video signals are acquired by a frame grabber board PicPort and image processing software HALCON. The sampling time of the controller is 0.2 [s]. The position, velocity and orientation of the vehicles are calculated by using the image processing.

To illustrate the enclosing performances of the proposed control law, the experiments are carried out in which 3 vehicles and one target-object with information exchange

TABLE II

Control parameters for experiments

k_i	0.3
k_c	1
r_d [m]	$[0.1, 0]$
R_i [m]	$\left[\cos\frac{\pi}{6}(i-1), \sin\frac{\pi}{6}(i-1)\right]$
v_{obj} [m/s]	0.04

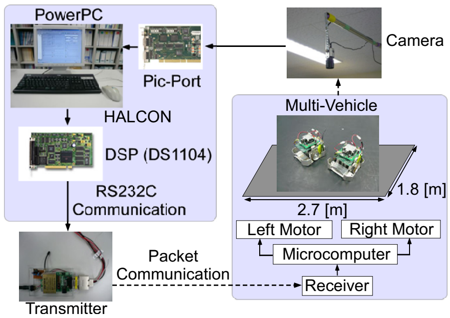

Fig. 5. Experimental setup

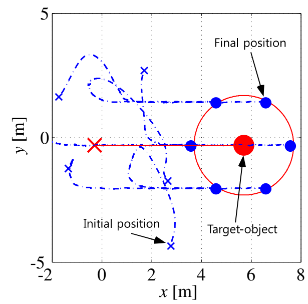

Fig. 6. Simulation results using (16): Trajectories of vehicles

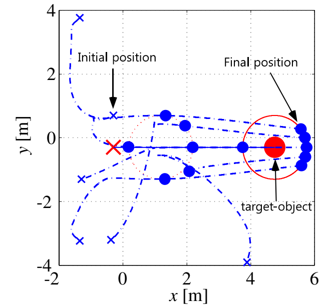

Fig. 7. Simulation results using (25)(26): Trajectories of vehicles

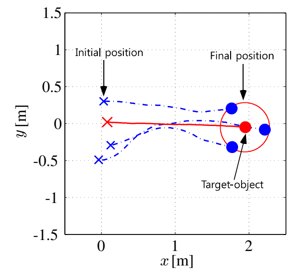

Fig. 8. Experimental results : Trajectories of vehicles and target-object

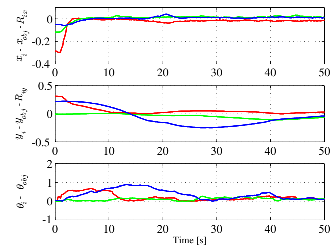

Fig. 9. Experimental results : Time plots of $\hat{r}_i - r_{obj}$ and $\theta_i - \theta_{obj}$

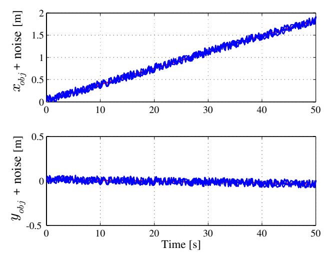

Fig. 10. Signal (x_{obj}, y_{obj}) with noise w_i

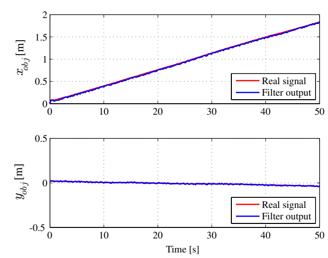

Fig. 11. Output (x_c) of the Consensus Filter

topology in Figure 4(b). The control parameters of the experiments are given as shown in Table II. The experiment results are shown in Figures 8-11. And, we set the covariance $W = 0.0024 I_2$ for all i. Figure 8 illustrates the trajectories of the three vehicles and the target object. Figure 9 illustrates $\hat{r}_i - r_{obj}$ and $\theta_i - \theta_{obj}$ of each vehicle. Fig. 10 shows the positions of the target-object that each vehicle obtains. Fig. 11 shows the positions of the consensus filter of each vehicle. From the experimental results, the control objectives C1)-C3) are achieved.

VII. Conclusions

In this paper, we proposed target-enclosing strategies using consensus filter for multiple nonholonomic vehicles which are controlled to converge to the formation while they are tracking the target-object moving in a plane. First, we defined a virtual vehicle in each vehicle to apply the consensus algorithm to nonholonomic vehicle, and linearized each vehicle. We propose the enclosing control law based on the consensus algorithm to each virtual vehicle. Then, the target-object was enclosed using the states of the consensus filter for the control law. Finally, the effectiveness of the proposal method was verified by the numerical simulations and the experiments.

References

[1] R. O. Saber, J. A. Fax and R. M. Murray: Consensus and Cooperation in Networked Multi-vehicle Systems, in *proc. IEEE*, Vol. 95, No. 1, pp. 215-233, 2007.

[2] V. Kumar, N. Leonard and A. S. Morse, eds.: *Cooperative Control, Lecture Notes in Control and Information Sciences*, Vol. 309, Springer, 2004.

[3] A. Jadbabaie, J. Lin, and A. S. Morse: Coordination of groups of mobile autonomous agents using nearest neighbor rules, *IEEE Trans. on Autom. Contr.*, Vol. 48, No. 6, pp. 988-1001, 2003.

[4] G. A. S. Pereira, V. Kumar and M. F. M. Campos: Decentralized Algorithms for Multi-Robot Manipulation via Caging. *The Int. J. of Robotics Research*, Vol. 23, No. 7, 2004.

[5] T. H. Kim and T. Sugie: Cooperative control for target-capturing task based on a cyclic pursuit strategy, *Automatica*, Vol. 43, Issue 8, pp. 1426-1431, 2007.

[6] Y. Kobayashi, K. Otsubo and S. Hosoe: Autonomous Decentralized Control of Capturing Behavior by Multiple Mobile Robots, *Trans. The Society of Instrument and Control Engineers (SICE)*, Vol. 43, pp. 663-671, 2007.

[7] D. J. Klein and K. A. Morgansen: Controlled Collective Motion for Trajectory Tracking, in *proc. Amer. Contr. Conf.*, pp. 5269-5275, 2006.

[8] S. Woo and S. Jayasuriya: Cooperative Surveillance of a Moving Target using a Formation Framework, in *proc. the 17th IFAC World Congress*, pp. 587-592, 2008.

[9] H. Yamaguchi: A distributed motion coordination strategy for multiple nonholonomic mobile robots in cooperative hunting operations, *Robot. Auton. Sys.*, Vol. 43, Issue 4, pp. 257-282, 2003.

[10] D. J. Klein, C. Matlack and K. A. Morgansen: Cooperative Target Tracking using Oscillator Models in Three Dimensions, in *proc. Amer. Contr. Conf.*, pp. 2569-2575, 2007.

[11] J. A. Marshall, M. E. Broucke and B. A. Francis: Formations of Vehicles in Cyclic Pursuit, *IEEE Trans. on Autom. Contr.*, Vol. 49, No. 11, pp. 1963-1974, 2004.

[12] W. Ren: Consensus Strategies for Cooperative Control of Vehicle Formations, *IET Control Theory & Applications*, Vol. 1, No. 2, pp. 505-512, 2007.

[13] W. Ren: Multi-vehicle Consensus with a Time-varying Reference State, *Sys. & Contr. Lett.*, Vol. 56, Issue 7-8, pp. 474-483, 2007.

[14] C. Yoshioka and T. Namerikawa: Formation Control of Nonholonomic Multi-vehicle Systems Based on Virtual Structure, in *proc. 17th IFAC World Congress*, pp. 5149-5154, 2008.

[15] H. Kawakami and T. Namerikawa: Virtual Structure Based Target-enclosing Strategies for Nonholonomic Agents, *in proc. IEEE Multi-conf. Sys. Contr.*, 2008. (to be presented)

[16] Z. Lin, B. Francis and M. Maggiore: Necessary and sufficient graphical conditions for formation control of unicycles, *IEEE Trans. on Autom. Contr.*, Vol. 50, No. 1, pp. 121-127, 2005.

[17] R. O. Saber and J. S. Shamma: Consensus Filters for Sensor Networks and Distributed Sensor Fusion, in *proc. IEEE Conf. Dec. Contr.*, pp. 6698-6703, 2005.

[18] Y. Sun and M. Lemmon: Convergence of Consensus Filtering under Network Throughput Limitations, in *proc. IEEE Conf. Dec. Contr.*, pp. 2277-2282, 2007.

[19] D. P. Spanos, R. O. Saber and R. M. Murray: Dynamic Consensus for Mobile Networks, in *proc. the 16th IFAC World Congress*, 2005.